

A critical role of Binary mixture of fatty acid-based PCM selection to optimize the panel temperature and analyzed the effect of PCM for the different climatic condition

P.Prasanna^a, R. Ramkumar^a, R. Rajaseakar^a

^aDepartment of Mechanical Engineering, Annamalai University, India

Abstract

The solar photovoltaic system demonstrates a good capability for grid-scale and dispatchable power generation. However, the voltage of the panel degrades at higher operating temperatures. A binary mixture of fatty acids was integrated on the back of a PV panel with 30 mm and 50 mm thickness, and its performance was compared to a panel without the PCM unit (reference panel) to achieve thermal regulation. In this study, it was observed that during the vernal equinox (March), the PR of the panel was as low as 70.3% on average, owing to its higher operating temperature, which is maximum at 65.58°C. For the desired location (Chidambaram, Tamil Nadu), the effects of temperature on electric parameters and efficiency were also examined for the vernal equinox, summer solstice, autumn equinox, and winter solstice. Consequently, the average PR and efficiency of the panel were computed. As compared to the reference panel, a PR increase of 1.74% and 2.92% was observed in March, 1.44% and 2.22% in June, 1.17% and 1.94% in September, and 1.66% and 2.04% in December, respectively. On average, panel efficiency increases from reference panel to 30mm PCM and 50mm PCM panels by 9.64% to 9.80% and 9.93% in March, 9.88% to 10.01% and 10.10% in June, 9.99 to 10.11%, and 10.19% in September, and 10.12 to 10.30% and 10.34% in December.

Introduction

Photovoltaic cells are a widely accepted futuristic renewable energy technology that generates electricity by converting light photons into electrons through an electronic process using semiconductor materials. Silicon wafer-based PV technology accounts for approximately 95% of total production, with peak laboratory efficiencies of 26.1%, 23.3%, and 21.2%, respectively, for Monocrystalline, Polycrystalline, and thin-film crystals [1]. Commercially available silicon wafer-based PV modules convert about 13% to 17% of their energy into electricity, with the remainder converted to heat, resulting in energy loss [2-4]. Additionally, the increase in internal charge carrier recombination rates decreases the open-circuit voltage, energy conversion efficiency, and output power of the PV cells. The temperature coefficient at standard testing conditions (STC) for the PV module power reduction ranges from 0.41%/°C to -0.5%/°C [5-7]. Photovoltaics perform better when the temperature of the PV panel is kept at an optimal level [8-9]. Cooling technologies such as active and passive cooling were used to regulate the temperature of the modules. Active cooling reduces panel temperature by up to 30 degrees Celsius while increasing electrical efficiency by up to 22% [10]. However, maintaining the coolant flow requires additional energy, which exceeds the energy saved by PV cooling.

The use of phase change materials (PCM) in passive cooling methods to regulate the temperature of PV panels has yielded positive results and has recently received increased interest from the PV community [11-16]. Thermal systems' effective operation relies on PCM's large storage space in a small volume and its ability to charge and discharge heat at a nearly constant temperature [17-19]. The rated temperature of a solar panel is 25°C. Therefore, keeping the operating temperature of the panel close to the rated temperature would result in a better electric performance. As a consequence, numerous studies determined that the PCM melting temperature should be close to the rated temperature. However, it will not produce good results in every specific location. In their study, Khanna et al. [20] reported that the PCM melting temperature is close to ambient, resulting in the PCM extracting heat at a higher rate, resulting in a larger amount of PCM required to cool the PV panel for an extended period. Melting temperatures ranging from 51°C to 57°C have been used in a small amount of research without proper selection criteria.

Huang et al. [21] investigated the use of phase-change materials to increase the electrical conversion efficiency of solar PV systems. PCM (GR40) is employed in the research, but it is ineffective because the temperature differences between the ambient temperature at the experimental location and the melting temperature of PCM are too wide. Indartono et al. [22] used yellowish petroleum jelly as the PCM to improve the overall performance of the PV panel in Indonesian weather conditions. The PCM phase transition mechanism failed in this case because the melting temperature of PCM and the back temperature of the panel is almost similar. Therefore, the PCM melting temperature must be below the PV module temperature. Waqas et al. [23] suggest that solidification temperatures of around 25°C may not be optimal for all locations, particularly during summer nights when ambient temperatures are high, inhibiting the complete solidification of PCM. The PCM transition temperature must be optimized with a higher average nighttime temperature to ensure PCM solidification. For successful heat removal, the PCM must solidify at night. Using the same PCM (OM29) in the summer and winter months, Rajvikram et al. [24] found a 10% improvement in electrical efficiency during the winter months due to a drop in the temperature of the PV-PCM module. PV module temperatures can be

decreased by up to 1.2°C using the OM29 before 08:30 in the summer, after that time the module's temperature cannot be lowered since it cannot store latent heat for an extended period.

Table 1 Investigation of the cooling of PVs under various outdoor conditions using a PCM method.

Authors	PCM Type/ Melting temperature(°C)	Duration, location and tilt angle(β_{α})	Performances Achieved	Key Finding
Salem Nijmeh. et.al, 2020[25]	BioPCM/ Melting point temperature 25°C	Annual/ Jordan $\beta_{\alpha}=26^{\circ}$	PV systems were enhanced with Bio-PCM, which increased power generation by 3.4%.	PV systems operate below the STC temperature in cold climates. According to the results, PCM has no benefit in cooling modules at low temperatures.
Vat Sun. et.al., 2020[26]	Rubitherm RT42	Annual/ Thailand $\beta_{\alpha}=10^{\circ}$	The average amount of electricity generated per year could increase by 4.3%.	With high ambient temperatures and high solar radiation intensity in April, a solar cell has the lowest efficiency. However, with low ambient temperatures and strong solar radiation in November, maximum efficiency was achieved.
Ramanan Pichandi. et.al., 2020[27]	Na2CO3. 10H2O-MgSO4. 7H2O eutectic PCM/ Melting temperature 35.6 °C	During summer/ India	PCM melting temperature is close to that of the ambient temperature and can lower the temperature of PV modules by an average of 2.33°C.	The melting point of PCM is close to the ambient temperature. As a result of the PCM reaching a completely molten state quickly, which takes place at 14:00, there is almost no heat transfer from the PV rear surface to the PCM.
Christopher J.Smith. et.al., 2014[28]	Organic PCM	Annual/ Different location	Energy output has increased in all locations over a reference system with no PCM, and in some locations by more than 6% per year.	Ambient temperature has a significant effect on a PCM's melting temperature; a hot climate will require a high PCM melting temperature, while a cool climate will encourage a low PCM melting temperature. Optimal PV/PCM cell performance can be attained by using a PCM that fully melts during the day and fully solidifies in the evening, utilizing the latent heat capacity of the phase change material.
Jiaxin Zhao. et.al., 2019[29]	Organic paraffin PCM20, PCM25, PCM30.	Annual/ China	Improvements in electricity production (2,46%) over the reference PV system (year-round)	PCMs with a high melting temperature range is usually effective in summer, but they are inefficient in winter because they do not melt in cold weather, causing the system temperature to be higher than that of the reference PV system. While PCM's melting range is low, it performs better in the winter because it is easily melted and cannot be recovered to a solid-state in the summer.
Feyza Bilgin. et.al., 2018[30]	Paraffin wax	Hot month (May) and cold month (December)/ (Ankara/ Mersin) $\beta_{\alpha}=30^{\circ}$	An average annual improvement of almost 1.59% in efficiency was achieved by reducing PV panel operating temperature from about 0.31°C to 10.26°C with an efficiency improvement ranging from 0.48% to 3.73%.	The optimal operating temperature for PV panels differs from that of winter to summer. Ultimately, differentiation is caused mainly by heat-rejecting from the PCM layer to its surroundings due to the higher ambient temperature. The performance of PV-PCM systems must therefore be improved by optimizing the thermal management of the PCM layer.
Jungwoo Park, et.al., 2014[31]	Paraffin wax/ Melting temperature 25 °C	Annual/ South Korea/ $\beta_{\alpha}=90^{\circ}$	Compared to the conventional PV module, the generated electrical power output increased by 0.5% annually.	Performances of PV-PCM is limited energy conversion because panels paced vertically its low High solar radiation. During winter differences of melting temperature of PCM and the surrounding temperature has large variation therefore heat transfer between PCM and panel. In October, the ambient temperature and PCM temperature are the same and there is very limited heat transfer occurs. It is inferred that melting temperature PCM should be higher than that of ambient temperature for thermal regulation of PV panel.
J.H.C. Hendricks, et.al., 2021[32]	RT-42 paraffin PCM	Summer and winter weather conditions/Egypt/ $\beta=30.5^{\circ}$	Solar PV-PCM and PV-PCM/AF systems improved their electrical efficiency by 9% and 14%, respectively, in the summer. Meanwhile, in the winter, they improved by 3.7% and 4.8%.	The temperature difference between the PCM melting point and the night minimum ambient temperature must be at least 5°C to ensure solidification. The maximum benefits can be obtained when the PCM melting point is 10 °C to 12 °C higher than the average minimum ambient temperature.
A.Hasan. et.al., 2017[33]	PCM RT42	Annual/ The United Arab Emirates.	PV temperature was lowered by 10.5°C on average during peak hours due to the PCM, resulting in a 5.9% growth in PV power output per year.	PCMs did not completely solidify in the summer due to higher ambient temperatures at night, which limited their effectiveness. During the winter, the PCM was unable to receive enough thermal energy to completely melt, which led to a reduction in cooling efficiency. Different melting temperature PCM is needed to overcome the above problem.
Rok Stropnik, et.al., 2016[34]	Paraffin organic type RT28	Annual, Slovenia	Compared with a typical PV module, 4.3–8.7% more electrical power was generated, increasing energy generation efficiency by 0.5–1%.	It was found that PV-PCM panel performances were limited from November to January when compared with conventional reference panels. A specific PCM was needed in those months to improve PV performances.

Table 1 shows some of the outcomes of a PCM-based experimental study on PV cooling in various outdoor conditions. According to the literature studies, the specific PCM material was not suitable for a whole year due to the hot and cold climatic conditions. Meanwhile, the generation of PV power will fluctuate depending on the climate. As a result, different melting temperatures of PCM material are required to lower the temperature produced by PV panels. Solar radiation combined with optimal panel operating temperature results in maximum efficiency. PV panels employ a PCM unit to reduce temperature. The maximum solar radiation is received when the panel is oriented perpendicular to the sun, and this angle is called the angle of inclination. Because of the rotation of the earth, the angle of inclination changes throughout the season. Above PV-PCM studies perform the same tilt angle of panels throughout the year. The tilt angle of the panel must be adjusted every month to improve panel performance.

The experimental set-up was established, and the entire experimental method was carried out in four different seasons of Indian weather conditions. The goal of this research is to investigate and compare the PV panel's performance under various operating situations. The PV-PCM system's advances have been analyzed and discussed. In addition, this system's economic analysis and carbon emissions were also discussed.

2. Mathematical calculation

2.1 Computation of the solar angle

It is highly recommended that the angle of inclination of solar panels be adjusted once a month to optimize photovoltaic production. A tilt of the Earth around the sun creates an angle between the sun's rays incident on the Earth, known as the declination angle (δ). This angle varies seasonally based on Earth's tilt about the sun. As January 1st is $D = 1$, D represents the day of the year [35].

$$\delta = -23.45 * \cos \left(\frac{360}{365} * (D + 10) \right) \quad (1)$$

The solar hour angle (ω_s) is the angle formed by the sun at solar noon and the sun at the local solar time. ϕ is the latitude of the desired location.

$$\omega_s = \cos^{-1}[-\tan(\phi) \tan(\delta)] \quad (2)$$

Solar panels' "tilt angle" - or "elevation angle" - are determined by their vertical angle concerning the sun. For the most efficient output, the solar panel should face directly into the sun [36].

$$\beta_\alpha = \phi - \tan^{-1} \left[\frac{\omega_s}{\sin \omega_s} \tan(\delta) \right] \quad (3)$$

2.2 Performances calculation

The system energy balance equation is used to calculate the rate of temperature change of a PV-PCM module, as shown in Equation (4).

$$\left\{ \begin{array}{l} \text{Rate of temperature} \\ \text{change of P panel} \end{array} \right\} = \left\{ \begin{array}{l} \text{i. Input solar} \\ \text{energy} \end{array} \right\} - \left\{ \begin{array}{l} \text{ii. Electrical} \\ \text{output} \end{array} \right\} - \left\{ \begin{array}{l} \text{iii. Mode of} \\ \text{heat transfer} \end{array} \right\} \quad (4)$$

i. Equation (5) gives the input solar energy (G). Where I_G is the solar radiation incident on the panel, A_{PV} is its area, and α is its absorptivity constant.

$$G = \alpha I_G A_{PV} \quad (5)$$

ii. Electrical energy output (P) from the PV panel is given by Equation (6):

$$P = V * I \quad (6)$$

The PV-PCM systems electrical efficiency is computed by

$$\eta_{elic} = \eta_{PV} [1 - \beta (T_{PV} - T_{STC})] \quad (7)$$

Where β is the temperature coefficient of the electrical efficiency (0.45%/°C) and T_{PV} , T_{STC} is the temperature of the PV panel and standard test condition temperature [37].

Performance Ratio (PR) is an authentic metric to analyze plant performance. It is a ratio of energy generated by insolation and its installed capacity in Equation (8)[38]. PR of one PV plant can be compared with another plant. It's a measure of the quality of PV plants that is independent of location. PR percentage defines the energy available to export after deduction of all the losses.

$$\text{Performance ratio (PR)} = \frac{P}{I_G \cdot A_{PV} \cdot \eta_{PV}} \quad (8)$$

Capacity Utilization Factor (CUF) or plant load factor is a metric used to estimate the plant available for generation over the period concerning its installed capacity [38].

$$CUF = \frac{\text{Energy}}{\text{Number of days} \cdot 24 \cdot \text{Installed capacity}} \quad (9)$$

iii. Figure 1 shows the mode of heat transfer that occurs in the PV-PCM system.

Conduction heat transfer (Q_{con}) between a PV module and a PCM, where k denotes thermal conductivity, x is the thickness of the PCM, and ΔL is the latent energy of the PCM.

$$(Q_{con}) = k A_{PV} x \Delta L (T_{PV} - T_{PCM}) \quad (10)$$

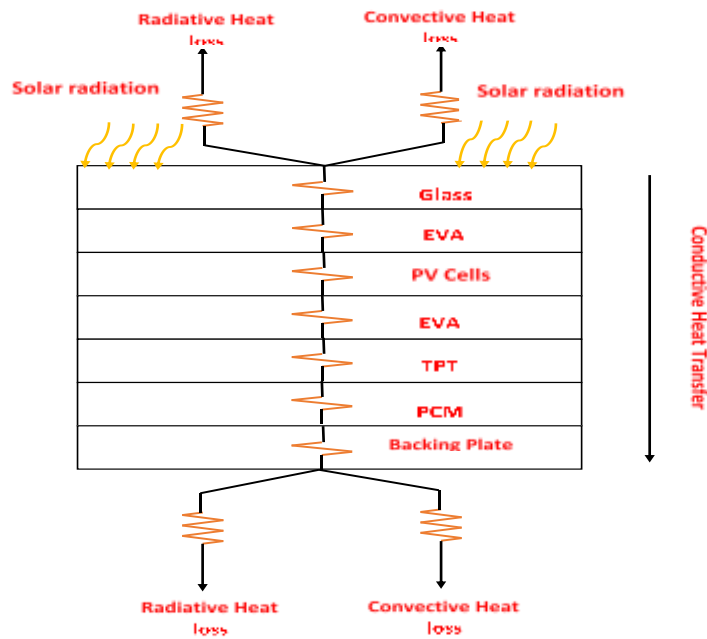


Figure 1 Schematic view of heat transfer mode for solar panel

The module net radiation heat transfer (Q_{rad}) is calculated as:

$$(Q_{rad}) = 2 h_r A (T_{PV} - T_{amb}) \quad (11)$$

Where σ is the Stefan-Boltzmann ($5.6693 \cdot 10^8 \text{ W/m}^2$) constant, h_r is a radiative heat transfer coefficient and ϵ_{PV} is the emissivity of the module [39].

$$h_r = \sigma \epsilon_{PV} (T_{PV}^2 + T_{sky}^2) (T_{PV} + T_{sky}) \quad (12)$$

Using a modified Swinbankequation T_{sky} is defined as the temperature of the sky.

$$T_{sky} = 0.037536 T_{amb}^{1.5} + 0.32 T_{amb} \quad (13)$$

Convective heat loss (Q_{conv}) of a panel is defined as

$$(Q_{conv}) = h_c A (T_{PV} - T_{amb}) \quad (14)$$

$$h_c = 5.7 + 3.8 v \quad (15)$$

Where the h_c heat loss coefficient and v is the wind velocity [40].

3. Experimental setup and Procedure.

3.1 Experiment set up

Three polycrystalline silicon solar panels rated at 5W are connected independently to a data acquisition system. In Figure 2, the first panel is a reference, whereas the other two panels are PV-PCM. Table 2 lists the electrical characteristics provided by the manufacturer for the PV panels.

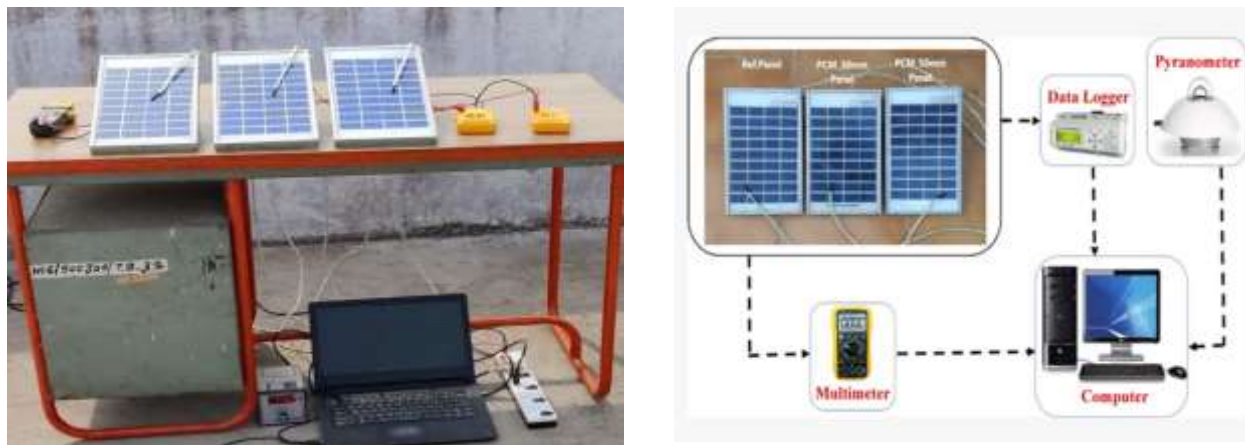


Figure 2 Schematic view of Experimental set-up and aluminum PCM Container

Figure 2 shows two PCM containers with thicknesses of 30 mm and 50 mm packed in the second and third panels, respectively (volumes of 230*136*30 and 230*136*50, all in mm) as depicted. For this study, the following assumptions were made:

- PV modules receive solar radiation evenly dispersed over their surface.
- The contact resistance of PV cells is not considered.
- In solid and liquid phases, PCMs possess homogeneous and isotropic characteristics.
- The flow of a molded PCM could be considered laminar and incompressible.

Table 2 Specification of Experimented PV panel

Specification	Unit	Value
Rated power	P_{max} (W)	5
Open circuit voltage	V_{oc} (V)	22.3
Short circuit current	I_{sc} (A)	0.3
Electrical Conversion Efficiency	η_{elic} (%)	11.5 at STC
Voltage at P_{max}	v_{mp} (V)	17.8
Current at P_{max}	I_{mp} (A)	0.28

3.2 Phase Change Material

From LOBA Chemie Pvt. Ltd., we purchased 99% lauric acid and 99% palmitic acid. A binary eutectic mixture was previously prepared at melting temperatures of 35 °C and 40 °C, which produced two distinct compositions (85:15 LA) and (69:31 LA), respectively. This combination of the binary eutectic mixture had good thermal stability and less correctional to encapsulation material such as copper, aluminum and stainless steel [41]. Table 2 shows the thermophysical properties of the fatty and prepared binary eutectic PCM. Chidambaram's climate was generally warmer and dryer between February and August, reaching an average temperature of 32.8°C and solar radiation of 717.44 W/m² on average. The cold weather between September and January had solar radiation of 628.77 W/m² and a temperature of 28.6°C [42]. There are many factors involved in choosing two different melting temperatures for PCM. The temperature difference between the melting point of the PCM and the minimum ambient temperature should be at least 5 °C [43, 44] to ensure solidification of the PCM at night. Accordingly, the melting temperature of eutectic PCM is 40 °C, when used in the warm months of March and June, whereas the melting temperature of eutectic PCM is 35 °C when used in the cold months of September and December.

Table 3 Thermophysical properties of PCM

Thermophysical properties of above fatty acid		
PCM	Lauric Acid	Palmitic Acid
Melting point(°c)	42	62
Latent of fusion (J.g ⁻¹)	175.8	212
Molecular weight	200.32	256.43
Molecular formula	C ₁₂ H ₂₄ O ₂	C ₁₆ H ₃₂ O ₂
Thermophysical properties of binary eutectic Fatty Acid		
Material ratio	69:31	85.5:14.5
Melting temperature (°c)	34.6	40.9
Latent heat of fusion(J/g)	195.49	174.54

Result:

In Annamalai University, Chidambaram (11.4070° N, 79.6912° E) in Indian weather conditions, a functioning prototype was built to assess the possibility of using a Phase Change Material with a PV panel. The experiments were conducted under the above weather conditions and the results obtained are shown in the following sections. The experiment has been carried out for the different climatic conditions of a single location to capture how seasonality affects the efficacy of a PCM. Four different months have been considered such as Vernal equinox (March), Summer solstice (June), Autumn equinox (September) and Winter solstice (December). These four months’ sun moves from tropic of cancer to the tropic of Capricorn.

4.1. Average irradiation and ambient temperature for Hot and cold month.

Solar radiation and ambient temperature were recorded in 15-minute time intervals during March and June, which were hot weather, respectively, and September and December in terms of cold weather. The average solar radiation and ambient temperature for March and June are illustrated in Figure 3, with a maximum of 908.68, 821.86 W/m², and 34.44 and 33.51°C, respectively. The average ambient temperature in March is increasing steadily, reaching its maximum temperature at noon, and from then on, the temperature is falling. For September and December, Figure 4 shows average solar irradiance and ambient heat of 780.09 and 786.37 W/m² with maximum temperatures of 33.51 and 33.76°C. The average temperature in September grows steadily, peaks at noon, stay at 14:00, and then drops. Likewise, the temperature reached its maximum at 13:00 in December, then fell from there shortly afterward.

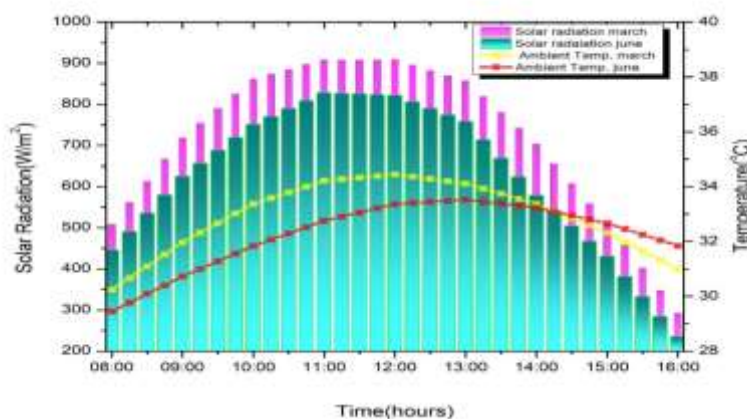


Figure 3 Average solar radiation and ambient temperature for hot months of March and June

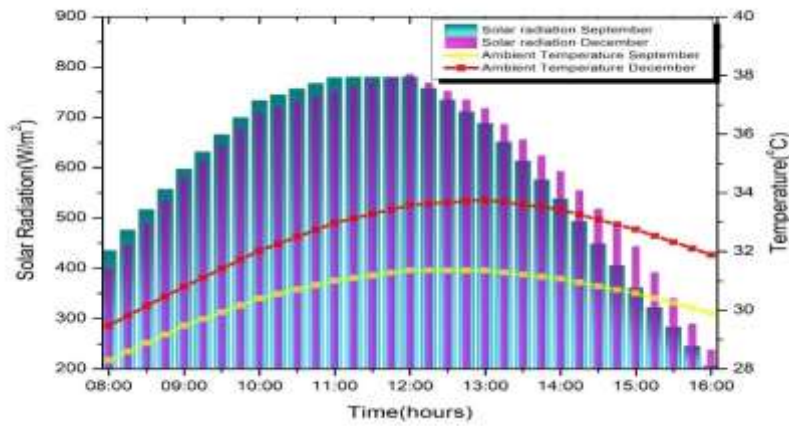


Figure : 4 Average solar radiation and ambient temperature for hot months of September and December

4.2 Monthly solar panel tilt angle

The sun must be directly perpendicular to the panels to generate the maximum amount of energy when the panels are angled. This angle of the sun varies depending on the latitude and season. Therefore, solar panels should be positioned for maximum exposure to solar intensity and should be adjusted according to the seasons. Table 4 depicts the monthly variation of the optimum tilt angle at Chidambaram (11.407° N, 79.6912° E). The tilt angle of -1.7° occurs in June, while the tilt angle of 28.3° occurs in December. Solar panels should face north when the tilt angle is negative. In seasonal optimum tilt angles, the monthly optimum tilt angles are averaged throughout a season, whereas annual optimum tilt angles are averaged over a year. The solar tilt angles during four different seasons are: the vernal equinox and the autumnal equinox are 13.3°, the summer solstice is -1.7°, and the winter solstice is 28.3°.

Table 4 Monthly, seasonal and year around optimum solar panel tilt angle

OPTIMUM SOLAR PANEL TILT ANGLE BY SEASON		OPTIMUM SOLAR PANEL TILT ANGLE BY MONTH	
Vernal Equinox (March)	13.3	January	23.3
Summer Solstice (June)	-1.7	February	18.3
Autumn Equinox (September)	13.3	March	13.3
Winter Solstice (December)	28.3	April	8.3
		May	3.3
		June	-1.7
		July	3.3
		August	8.3
		September	13.3
		October	18.3
		November	23.3
		December	28.3
OPTIMUM YEAR AROUND SOLAR PANEL TILT ANGLE			
13.3			

4.2 Effect of Temperature on reference and PCM panel

Comparison of the reference PV and PV-PCMs panels from the perspective of performance. In figures 5 and 6, average temperatures for 30mm and 50mm thick PCM equipped panels and a reference PV panel temperature are plotted for hot (March and June) and cold (September and December) climatic conditions. The data are plotted only during sunshine hours from 8:00 AM to 16:00. As a reference panel does not contain a heating unit, the maximum temperature recorded during March is 58.16°C, and the minimum temperature recorded for a panel with 50mm thickness PCM during September is 34.54°C. Figure 5 shows that the

temperature of the Post noon at 14:15 reference panel drops less than that of the 30 mm PCM panel and the 50 mm PCM panel as forced convective heat transfer takes place when the PCM panel is integrated.

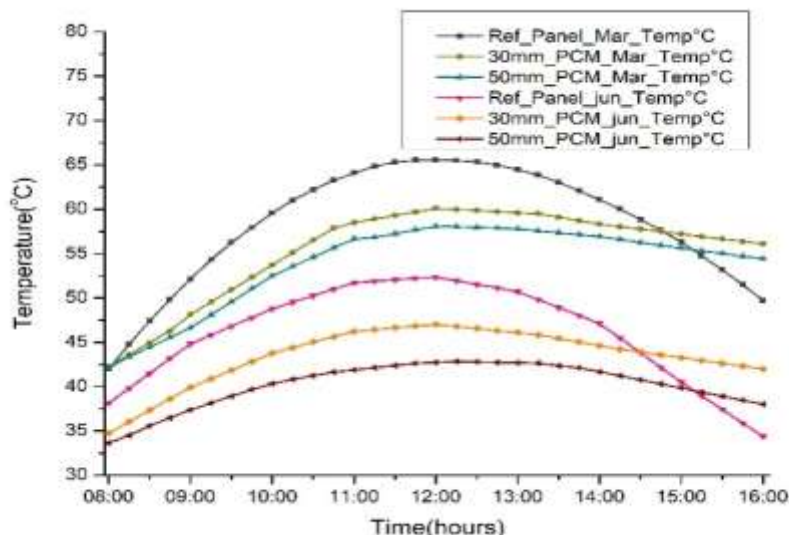


Figure 5 Average Temperature of Hot months

For March, June, September and December, the average reference panel temperatures are 52.34°C, 46.44°C, 44.05°C and 47.46°C, respectively. By adding a PCM unit, the reference panel temperatures were reduced to 48.59°C, 43.63°C, 42.58°C, and 42.95°C, respectively, when using 30 mm thick PCM. The panel temperature was further lowered with 50mm of PCM to 46.41°C, 41.84°C, 40.96°C, and 41.16°C, which was close to the NOCT (45°C). In this case, as well, a 50mm PCM panel would incur less energy loss because the panels were working at a lower temperature. In terms of temperature dissipation, a 50 mm thick PCM dissipated 11.61%, 9.9%, 7.01%, and 13.21% more heat than a reference panel during March, June, September, and December, respectively.

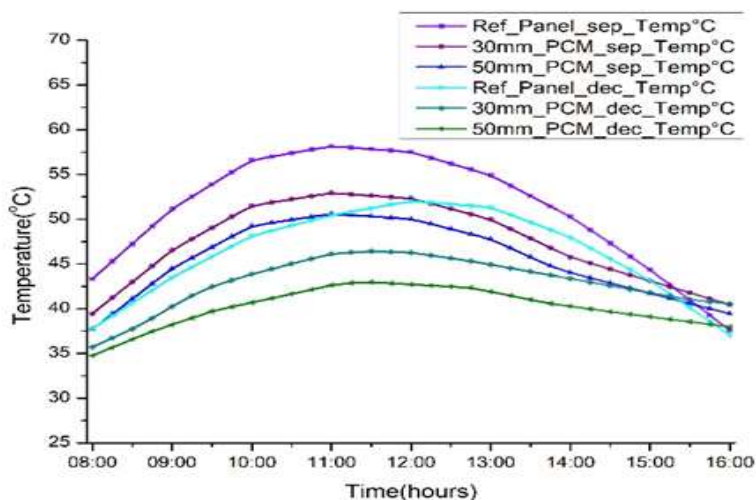


Figure 6 Average Temperature of cold months

4.3 Effect of climate on reference and PCM panel

For hot and cold climatic conditions in March, June, September, and December, the average power of a reference panel, 30mm and 50mm thick PCM equipped panels, is plotted in Figure 7. Reference panels produced an average power of 2.62W, 2.35W, 2.22W and 2.24W, respectively. Adding the PCM unit had increased the power output to 2.67W, 2.39W, 2.25W, and 2.29W, respectively for 30 mm thick PCM. The panel power was further increased by adding 50mm of PCM to achieve 2.71W, 2.41W, 2.27 W, and 2.32 W, respectively. The cloudy event caused a minor dip in power generation at 12:15. During the period of experimentation, there were no fluctuations in electrical power, meaning there were not many cloudy days. Since March had more irradiation than December, it had recorded more electrical power. PCM was effective at 50 mm thickness since it dissipated 9.98%, 9.99%, 1.988%, and 3.053% more power, respectively, in March, June, September, and December.

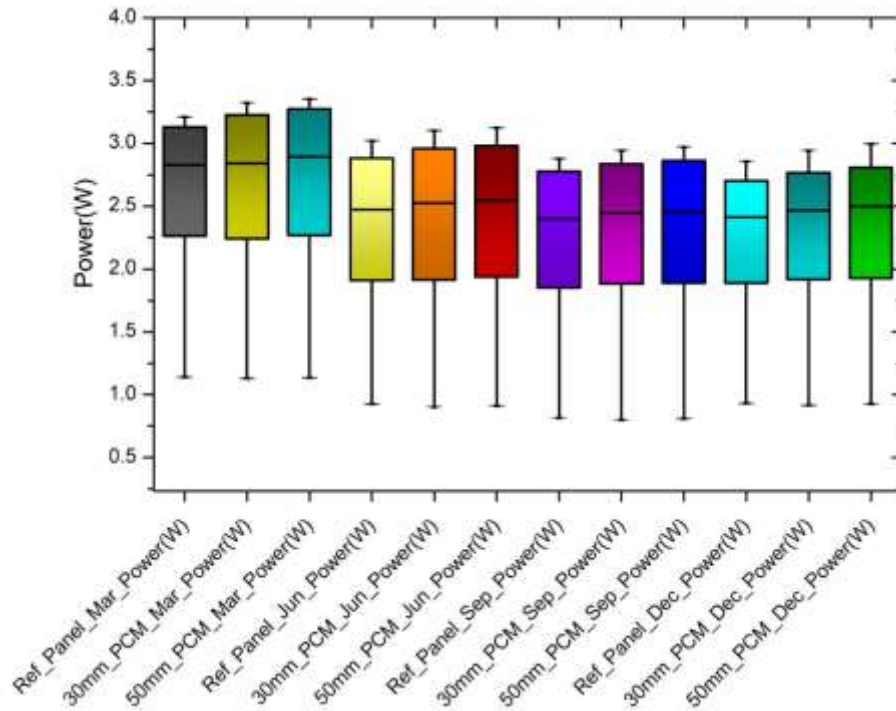


Figure 7 Distribution of PCM Power at different thicknesses and Reference panel power

4.4 Effect of climate on electrical efficiency.

Figure 8 shows the average efficiency of the reference panel, 30mm and 50mm thick PCM equipped panels in hot and cold climatic conditions. A panel with a 50mm thickness PCM can achieve maximum average efficiency of 6.64% in December, while a reference panel without a heating unit can achieve a minimum average efficiency of 9.64% in March. During March, June, September, and December, the average efficiency of the reference panel was 9.64%, 9.88%, 9.99%, and 10.12%. With the addition of the 30mm PCM unit, the reference panel's efficiency increased to 9.8%, 10.01%, 10.11%, and 10.3%, respectively. With the addition of a 50mm PCM panel, the panel's efficiency increased even further to 9.93%, 10.10%, 10.19%, and 10.34%.

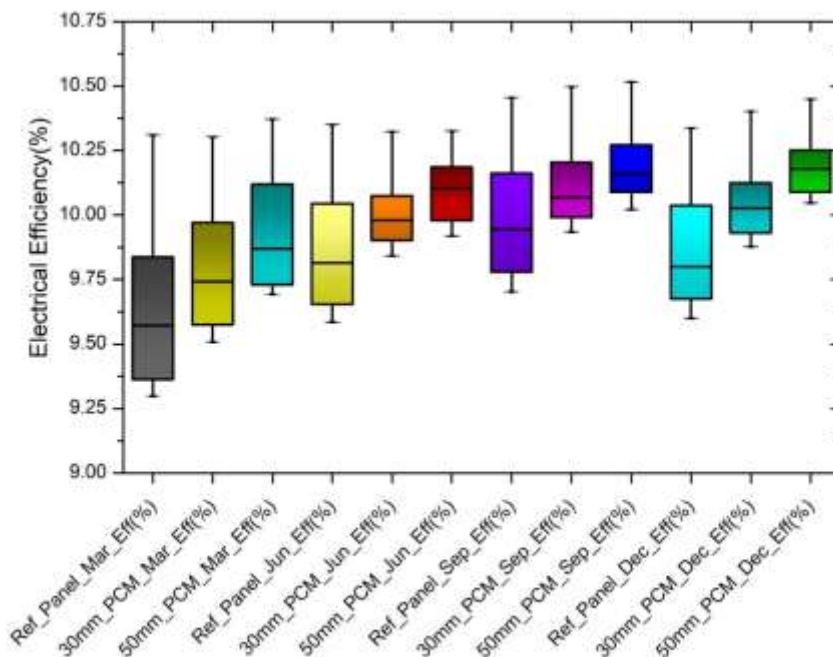


Figure 8 Distribution of PCM Efficiency at different thicknesses and Reference panel efficiency

To achieve both economic and electrical performance goals, the PCM was incorporated into the solar PV panel. Due to the reduced operating temperature, high-efficiency panels are possible. For the five-watt solar photovoltaic system, Table 5 shows the parameters for three different panel types: the reference panel, the PCM integrated panel in 30mm and 50mm thickness, and for four different months (March, June, September, and December).

Table 5Electrical parametric performances

<i>Month</i>	<i>Power</i>	<i>PR</i>	<i>P_{nom}</i>	<i>P_{loss}</i>	<i>Efficiency</i>	<i>CUF</i>
March						
Reference	2.622	0.730	2.997	0.375	9.64%	17.300
30_mm PCM panel	2.676	0.743	2.997	0.321	9.80%	17.650
50_mm PCM panel	2.711	0.752	2.997	0.286	9.93%	17.890
June						
Reference	2.352	0.748	2.619	0.267	9.88%	15.52
30_mm PCM panel	2.394	0.759	2.619	0.225	10.01%	15.8
50_mm PCM panel	2.415	0.765	2.619	0.205	10.10%	15.93
September						
Reference	2.224	0.757	2.448	0.224	9.99%	14.67
30_mm PCM panel	2.259	0.766	2.448	0.189	10.11%	14.9
50_mm PCM panel	2.277	0.772	2.448	0.171	10.19%	15.02
December						
Reference	2.260	0.767	2.454	0.195	10.12%	14.91
30_mm PCM panel	2.304	0.780	2.454	0.151	10.30%	15.2
50_mm PCM panel	2.320	0.783	2.454	0.134	10.34%	15.31

In Table 5, March has the highest average power because radiation levels were higher during the test period compared with the other three months preceding it. According to this report, the 50mm PCM panel produced more power during March, June, September, and December than the other panels, which produced 3.024W, 2.958W, 2.706W, and 2.294W, respectively. For a 50mm PCM panel, the highest CUF (%) was obtained. Because of the higher intensity of 7.236 KWh/m² and the effective thickness of the PCM, it was 19.96% in March. However, during June, September, and December, it was 19.53 %, 17.83 %, and 15.14 %, respectively. Despite its greater PR value, December CUF is lower due to its lower intensity of 6.042 KWh/m². In December and June; the panel performance (PR) outperforms the PR estimated in the other experimental months. The loss due to temperature was lower in December owing to the winter solstice, while the longest sunny days occurred in June for the summer solstice. In March, compared to December and June, PR was significantly lower, at 6.5% and 5.1%, respectively. It is critical to note that the PR value of the 50mm PCM panel was greater than that of the 30mm PCM panel and the reference panel in four months.

The panel standard efficiency is 11.5 % (STC). In March, June, September, and December, the reference panel's average efficiency was lowered to 9.28%, 9.88%, 9.63%, and 10.18%, respectively, according to Table:4. By combining PCM at 30mm thickness and PCM at 50mm thickness, the efficiency was increased to 9.42%, 10.01%, 9.81%, and 10.30%, respectively, 9.50%, 10.17%, 9.91%, and 10.35%. Because the ambient temperature was lower in December, the panel performed close to the efficiency of the panel at STC, with a peak efficiency of 10.35% for the 50mm PCM panel.

Table 6Thermal parametric performances

<i>Month</i>	<i>hc</i>	<i>hr</i>	<i>T_{sky}</i>	<i>Q_{cov}</i>	<i>Q_{rad}</i>	<i>Q_{con}</i>	<i>Q_{Total}</i>
March							
30_mm PCM panel	2.174	0.008	17.636	1.0996	0.0045	3.849	4.953
50_mm PCM panel	2.078	0.007	17.636	0.8763	0.0032	5.295	6.174
June							
30_mm PCM panel	1.950	0.006	17.254	0.6133	0.0018	3.029	3.789
50_mm PCM panel	1.952	0.006	17.254	0.6240	0.0019	4.065	5.937

September							
30_mm PCM panel	2.022	0.006	16.085	0.7524	0.0021	2.663	3.277
50_mm PCM panel	1.945	0.005	16.085	0.6174	0.0016	3.891	4.421
December							
30_mm PCM panel	2.165	0.006	14.834	1.0458	0.0029	1.601	3.136
50_mm PCM panel	2.054	0.005	14.834	0.7988	0.0019	2.652	3.020

The total heat removed from the experimental system for both the 30mm PCM panel and the 50mm PCM panel is 4.953J, 3.789J, 3.277J, 3.136J and 6.174J, 5.937J, 4.421J, 3.020J for the respective months, respectively. From the table, it is clear that conductive and radiation heat losses are quite high for the 30mm PCM panel compared to the 50mm PCM panel. Because the temperature of the PV panel is quite high for a 50mm PCM panel. Solar radiation is high during March and the ambient temperature is low during December. So the temperature difference between the PV panel and ambient temperature influences the increase in conductive and radiation heat transfer losses. In this study, useful heat was stored by a conduction heat transfer mechanism using Phase Change Material. From the table, the heat stored through conduction for the 30mm PCM panel and 50mm PCM panel is 3.849J, 3.029J, 2.663J, 1.601J and 5.295J, 4.065J, 3.891J, and 2.652J. In December, conduction heat storage is less. Because the PV panel temperature is lower during December, this is due to metrological conditions experimentallocation.

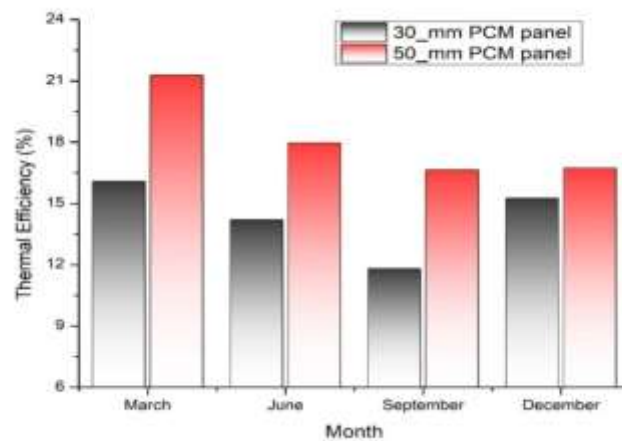


Figure 9 Thermal efficiency of PV-PCM panel

Figure 9 shows the average panel thermal efficiency of a 30 mm PCM panel and 50 mm PCM panel stored heat utilizing PCM employing the conduction heat transfer technique during solstice and equinox months. PCM was incorporated at an appropriate thickness to allow the heat dissipation as forced convective heat transfer happens tremendously. During the daylight hours, the thermal efficiency was calculated. For the relevant months, the average efficiency from a 30mm PCM and 50mm PCM panel was 16.07%, 14.19%, 11.80%, 15.02%, and 21.27%, 17.97%, 16.63%, 16.73%. A spacing of 50 mm is more efficient and optimal. In September, the 30mm PCM panel had a minimum efficiency of 11.80 %, while the 50mm PCM panel had a minimum efficiency of 16.63 %. Because rain occurs in this session most of the time, solar production is null during those days. As a result, this month's average production for both thermal and electrical efficiency minima.

Economic analysis

PV-PCM systems come with three major costs: (i) cost of the PCM, (ii) PCM containment materials, and (iii) fabrication costs. The PCMs were bought in smaller quantities (LOBA Chemie Pvt. Ltd.) for 13.69 USD/kg for LA and 10.74 USD/kg for PA. According to the ICIS pricing, LA costs will decrease by 0.71 USD/kg and PA costs will decrease by 0.79 USD/kg if purchased in large quantities[45]. PCM layers of 30 mm and 50 mm thickness require 0.776 kg and 1.372 kg of eutectic PCM, respectively. Table 7 shows the economic analysis of prepared Eutectic PCM.

PCM ratio (%)	PCM CombinationRatio (gram)		Experimental PCM Cost (USD)		ICIS cost (USD)	
	30mm PV-PCM	50mm PV-PCM	30mm PV-PCM	50mm PV- PCM	30mm PV- PCM	50mm PV-PCM
85 % of LA:15% of PA	659.6:116.4	1166:205	10.28	18.16	0.55	0.98
69 % of LA:31% of PA	535:240	946:425	9.90	17.50	0.54	0.96

The analysis uses two different aluminum containers, and the cost of material is based on the London Metal Exchange, which was around 0.80 USD [46]. In this study, a 5W module is used, so the additional cost incurred is estimated to be 4.5 USD/Wp and 0.54 USD/Wp for single-fabrication and mass-produced systems, respectively. During the month of testing, 30mm PV-PCM panels provided an average energy gain of 2.676W, 2.394W, 2.259W, and 2.304W and 50mm PV-PCM panels provided an average energy gain of 2.711W, 2.415W, 2.277W, and 2.32W. Using PV systems in India at 0.793 USD per Watt, the economic benefits are estimated. Financially, the 30mm PV-PCM system gains 2,12, 1,89, 1,79, and 1,82 USD from energy gains. According to the energy gains, the prices for the 50mm PV-PCM system are 2.14, 1.91, 1.8, and 1.83 USD. PV-PCM systems provide nearly equal economic benefits to the PCM setup if mass-produced. In addition, it may not be economically worthwhile to further increase the PCM layer thickness to control the PV module temperature. However, temperature regulation may result in a 20% increase in the lifespan of the PV module [47]. This can be considered helpful in places with similar climatic conditions to India.

Conclusion:

The performance of PV-PCM panels was compared to the unmodified PV panel during the summer solstice (June), the winter solstice (December), autumn equinox (September), and vernal equinox month (March). Due to effective convective heat transfer, the efficiency of the panels was increased from 9.64 to 9.8 and 9.93% by incorporating PCM at 30 mm and 50 mm thicknesses in March. In June, the panel's efficiency was 9.88%. When the 30mm and 50mm PCM panels were integrated, the efficiency improved to 10.01% and 10.10%. In September, the reference panel showed an efficiency of 9.99%, but with the integration of a 30mm and 50mm PCM panel, it rose to 10.11% and 10.19%. Using PCM at 30mm and 50mm thickness, the panel's efficiency increased from 10.12% to 10.30% and 10.34% in December. Compared to the reference panel, the efficiency of the 50mm PCM panel increased by 2.92 % in March, 2.17 % in June, 1.96 % in September, and 2.12 % in December. According to the study, binary mixture PCM in the ratio was extremely effective during the warmest months of the season. Furthermore, the related electrical and thermal properties were calculated and compared to a panel without PCM.

References

1. Best Research-Cell Efficiency Chart. (n.d.). Photovoltaic Research | NREL. Retrieved May 17, 2021, from <https://www.nrel.gov/pv/cell-efficiency.html>
2. S. Nizetic, E. Giama, A.M. Papadopoulos, Comprehensive analysis and general economic-environmental evaluation of cooling techniques for photovoltaic panels, Part II: active cooling techniques, *Energy Convers. Manag.* 155 (July 2017) 301e323. Jan. 2018.
3. Chandrasekar, M., & Senthilkumar, T. (2015). Experimental demonstration of enhanced solar energy utilization in flat PV (photovoltaic) modules cooled by heat spreaders in conjunction with cotton wick structures. *Energy*, 90, 1401-1410.
4. Usama Siddiqui, M., Arif, Arif.F.M., Kelley, L., Dubowsky, S., 2012. Three-dimensional thermal modeling of a photovoltaic module under varying conditions. *Sol. Energy* 86, 2620–2631.
5. Emam M, Ookawara S, Ahmed M. Performance study and analysis of an inclined concentrated photovoltaic-phase change material system.
6. Chow TT. A review on photovoltaic/thermal hybrid solar technology. *Appl Energy* 2010;87:365e79.
7. Cuce, P.M., Cuce, E., 2013. Improving thermodynamic performance parameters of silicon photovoltaic cells via air cooling. *International Journal of Ambient Energy*. Taylor & Francis Group
8. Radziemska E. The effect of power on the power drop in crystalline silicon solar cells. *Renew Energy* 2003;28(1):1–12
9. Hussain, S. Imran, R. Dinesh, A. Ameelia Roseline, S. Dhivya, and S. Kalaiselvam. 2017. "Enhanced Thermal Performance and Study the Influence of Sub Cooling on Activated Carbon Dispersed Eutectic PCM for Cold Storage applications." *Energy and Buildings* 143: 17–24. doi:10.1016/j.enbuild.2017.03.011.
10. Kibria, M. A., R. Saidur, F. A. Al-Sulaiman, M. D. Maniruzzaman, and A. Aziz. 2016. "Development of a Thermal Model for a Hybrid Photovoltaic Module and Phase Change Materials Storage Integrated in Buildings." *Solar Energy* 124: 114–123. doi:10.1016/j.solener.2015.11.027.

11. Wenyue, Lina, Zhenjun Ma, Paul Cooper, M. ImrozSohela, LuweiYangba. 2016. Sustainable. Thermal performance investigation and optimization of buildings with integrated phase change materials and solar photovoltaic thermal collectors. *Energy and Buildings* 116, 562–573.
12. Huang, M.J., Eames, P.C., Norton, B., 2006. Phase change materials for limiting power rise in building-integrated photovoltaics. *Sol. Energy* 80, 1121–1130. <https://doi.org/10.1016/j.solener.2005.10.006>.
13. Atkin, P., Farid, M.M., 2015. Improving the efficiency of photovoltaic cells using PCM infused graphite and aluminum fins. *Sol. Energy* 114, 217–228. <https://doi.org/10.1016/j.solener.2015.01.037>.
14. Sharma S, Tahir A, Reddy KS, Mallick TK. Performance enhancement of a building integrated concentrating photovoltaic system using phase change material. *Solar Energy Mater Sol Cells* 2016;149:29–39.
15. Sardarabadi, M., Passandideh-Fard, M., Maghrebi, M.-J., Ghazikhani, M., 2017. Experimental study of using both ZnO/water nanofluid and phase change material (PCM) in photovoltaic thermal systems. *Solar Energy Mater. Sol. Cells* 161. <https://doi.org/10.1016/j.solmat.2016.11.032>.
16. Kahwaji, Samer, and Mary Anne White. 2018. “Prediction of the Properties of Eutectic Fatty Acid Phase Change Materials.” *Thermochimica Acta* 660: 94–100. doi:10.1016/j.tca.2017.12.024.
17. Kauranen, P., K. Peippo, and P. D. Lund. 1991. “An Organic PCM Storage System with Adjustable Melting Temperature.” *Solar Energy* 46 (5): 275–278. doi:10.1016/0038-092X(91)90094-D.
18. Ma, Yanhong, Shiding Sun, Jianguo Li, and Guoyi Tang. 2014. “Preparation and Thermal Reliabilities of Microencapsulated Phase Change Materials with Binary Cores and Acrylate-Based Polymer Shells.” *Thermochimica Acta* 588: 38–46. doi:10.1016/j.tca.2014.04.023.
19. Huang, M. J., P. C. Eames, and Brian Norton. 2006. “Phase Change Materials for Limiting Temperature Rise in Building Photovoltaics.” *Solar Energy* 80 (9): 1121–1130. doi:10.1016/j.solener.2005.10.006.
20. Indartono, Y.S., Suwono, A., Pratama, F.Y., 2016. Improving photovoltaic performance by using yellow petroleum jelly as a phase change material. *Int. J. Low-Carbon Technol.* 11, 333–337. <https://doi.org/10.1093/ijlct/ctu033>.
21. Hasan, Ahmad, Sarah McCormack, Ming Huang, and Brian Norton. 2014. “Energy and Cost Saving of a Photovoltaic-Phase Change Materials (PV-PCM) System Through Temperature Regulation and Performance Enhancement of Photovoltaics.” *Energies* 7 (3): 1318–1331. doi:10.3390/en7031318.
22. Kibria, M. A., R. Saidur, F. A. Al-Sulaiman, M. D. Maniruzzaman, and A. Aziz. 2016. “Development of a Thermal Model for a Hybrid Photovoltaic Module and Phase Change Materials Storage Integrated in Buildings.” *Solar Energy* 124: 114–123. doi:10.1016/j.solener.2015.11.027.
23. Waqas, A., and J. Ji. 2017. “Thermal Management of Conventional PV Panel Using PCM with Movable Shutters – A Numerical Study.” *Solar Energy* 158: 797–807.
24. Rajvikram, M., S. Leponraj, S. Ramkumar, H. Akshaya, and A. Dheeraj. 2019. “Experimental Investigation on the Abatement of Operating Temperature in Solar Photovoltaic Panel Using PCM and Aluminium.” *Solar Energy* 188: 327–338. doi:10.1016/j.solener.2019.05.067.
25. Nijmeh, S., Hammad, B., Al-Abed, M., & Bani-Khalid, R. (2020). A Technical and Economic Study of a Photovoltaic-phase Change Material (PV-PCM) System in Jordan. *Jordan Journal of Mechanical & Industrial Engineering*, 14(4).
26. Sun, V., Asanakham, A., Deethayat, T., & Kiatsiriroat, T. (2020). Increase of power generation from solar cell module by controlling its module temperature with phase change material. *Journal of Mechanical Science and Technology*, 34, 2609–2618.
27. Pichandi, R., MurugavelKulandaivelu, K., Alagar, K., Dhevaguru, H. K., & Ganesamoorthy, S. (2020). Performance enhancement of photovoltaic module by integrating eutectic inorganic phase change material. *Energy Sources, Part A: Recovery, Utilization, and Environmental Effects*, 1-18.
28. Smith, C. J., Forster, P. M., & Crook, R. (2014). Global analysis of photovoltaic energy output enhanced by phase change material cooling. *Applied energy*, 126, 21-28.
29. Zhao, J., Ma, T., Li, Z., & Song, A. (2019). Year-round performance analysis of a photovoltaic panel coupled with phase change material. *Applied Energy*, 245, 51-64.
30. Arıcı, M., Bilgin, F., Nižetić, S., & Papadopoulos, A. M. (2018). Phase change material-based cooling of photovoltaic panel: A simplified numerical model for the optimization of the phase change material layer and general economic evaluation. *Journal of Cleaner Production*, 189, 738-745.
31. Park, J., Kim, T., & Leigh, S. B. (2014). Application of phase-change material to improve the electrical performance of vertical-building-added photovoltaics considering the annual weather conditions. *Solar Energy*, 105, 561-574.
32. Yousef, M. S., Sharaf, M., & Huzayyin, A. S. (2022). Energy, exergy, economic, and enviro-economic assessment of a photovoltaic module incorporated with a paraffin-metal foam composite: An experimental study. *Energy*, 238, 121807.
33. Hasan, A., Sarwar, J., Alnoman, H., & Abdelbaqi, E. S. (2017). Yearly energy performance of a photovoltaic-phase change material (PV-PCM) system in a hot climate. *Solar Energy*, 146, 417-429.
34. Strith, U. (2016). Increasing the efficiency of PV panels with the use of PCM. *Renewable Energy*, 97, 671-679.
35. Howell JR, Bannerot RB, Vliet GC. Solar-thermal energy systems analysis and design. New York: McGraw-Hill, Inc.; 1982.
36. Duffie JA, Beckman WA. Solar engineering of thermal processes. New York: Wiley; 1991.
37. Tiwari, Arvind, and M. S. Sodha. 2006. “Performance Evaluation of Hybrid PV/Thermal Water/Air Heating System: A Parametric Study.” *Renewable Energy* 31 (15): 2460–2474. doi:10.1016/j.renene.2005.12.002.
38. Kumar, B. Shiva, and K. Sudhakar. 2015. “Performance Evaluation of 10 MW Grid Connected Solar Photovoltaic Power Plant in India.” *Energy Reports* 1: 184–192. doi:10.1016/j.egyr.2015.10.001.

39. Hendricks, J. H. C., and W. G. J. H. M. Van Sark. 2013. "Annual Performance Enhancement of Building Integrated Photovoltaic Modules by Applying Phase Change Materials." *Progress in Photovoltaics: Research and Applications* 21 (4): 620–630. doi:10.1002/pip.1240.
40. Bayrak, Fatih, and Hakan F. Oztup. 2020. "Effects of Static and Dynamic Shading on Thermodynamic and Electrical Performance for Photovoltaic Panels." *Applied Thermal Engineering* 169: 114900.
41. P.Prasannaa, R. Rajasekar, R. Ramkumar. (2021). Evaluation of Thermal Reliability and Compatibility Analysis for Solar PV Cooling Applications by Using Binary Eutectic Fatty Acid as PCMs. *Design Engineering*, 11731 - 11743. <http://www.thedesignengineering.com/index.php/DE/article/view/6244>.
42. Prasannaa, P., Ramkumar, R., Sunilkumar, K., & Rajasekar, R. (2021). Experimental study on a binary mixture ratio of fatty acid-based PCM integrated to PV panel for thermal regulation on a hot and cold month. *International Journal of Sustainable Energy*, 40(3), 218-234.
43. Waqas, A., Jie, J., & Xu, L. (2017). Thermal behavior of a PV panel integrated with PCM-filled metallic tubes: An experimental study. *Journal of Renewable and Sustainable Energy*, 9(5), 053504.
44. Yousef, M. S., Sharaf, M., & Huzayyin, A. S. (2022). Energy, exergy, economic, and enviro-economic assessment of a photovoltaic module incorporated with a paraffin-metal foam composite: An experimental study. *Energy*, 238, 121807.
45. Independent commodity intelligence services (n.d.). <https://Www.Icis.Com/Explore/Services/Pricing-Intelligence/>. Retrieved January 19, 2022, from <https://www.icis.com/explore/services/pricing-intelligence/>
46. LME Aluminium | London Metal Exchange. (n.d.). Lme. Retrieved January 19, 2022, https://www.lme.com/Metals/Non-ferrous/LME_Aluminium#Trading+day+summary.
47. Savvakis, N., & Tsoutsos, T. (2021). Theoretical design and experimental evaluation of a PV+ PCM system in the mediterranean climate. *Energy*, 220, 119690.
48. Thangam, D., Malali, A. B., Subramanian, G., Mariappan, S., Mohan, S., & Park, J. Y. (2022). Relevance of Artificial Intelligence in Modern Healthcare. In *Integrating AI in IoT Analytics on the Cloud for Healthcare Applications* (pp. 67-88). IGI Global.
49. Thangam, D., Malali, A. B., Subramanian, G., Mohan, S., & Park, J. Y. (2022). Internet of Things: A Smart Technology for Healthcare Industries. In *Healthcare Systems and Health Informatics* (pp. 3-15). CRC Press.
50. Thangam, D., Malali, A. B., Subramanian, S. G., Mariappan, S., Mohan, S., & Park, J. Y. (2021). Blockchain Technology and Its Brunt on Digital Marketing. In *Blockchain Technology and Applications for Digital Marketing* (pp. 1-15). IGI Global.